BJ www.biochemj.org

Biochem. J. (2011) **440**, 251–262 (Printed in Great Britain) doi:10.1042/BJ20100739

online data

A novel protein from the serum of *Python sebae*, structurally homologous with type-γ phospholipase A_2 inhibitor, displays antitumour activity

Sandra DONNINI*, Federica FINETTI*, Simona FRANCESE†, Francesca BOSCARO‡, Francesca R. DANI‡, Fabio MASET§, Roberta FRASSON§, Michele PALMIERI*, Mario PAZZAGLI‖, Vincenzo DE FILIPPIS§, Enrico GARACI¶ and Marina ZICHE*[1]

*Department of Biotechnology and Istituto Toscano Tumori (ITT), University of Siena, Via A. Moro 2, 53100 Siena, Italy, †Biomedical Research Centre, Sheffield Hallam University, Howard Street, Sheffield, S1 1WT, U.K., ‡Mass Spectrometry Center (C.I.S.M.), Viale Pieraccini 6, 50139 Florence, Italy, §Department of Pharmaceutical Sciences, University of Padua, Via F. Marzolo 5, 35130 Padua, Italy, ‖Department of Clinical Physiopathology, University of Florence, Viale Pieraccini 6, 50139 Florence, Italy, and ¶Department of Experimental Medicine and Biochemical Sciences, University of Rome 'Tor Vergata', Viale Regina Elena 299, 00133 Rome, Italy.

Cytotoxic and antitumour factors have been documented in the venom of snakes, although little information is available on the identification of cytotoxic products in snake serum. In the present study, we purified and characterized a new cytotoxic factor from serum of the non-venomous African rock python (*Python sebae*), endowed with antitumour activity. PSS (*P. sebae* serum) exerted a cytotoxic activity and reduced dose-dependently the viability of several different tumour cell lines. In a model of human squamous cell carcinoma xenograft (A431), subcutaneous injection of PSS in proximity of the tumour mass reduced the tumour volume by 20 %. Fractionation of PSS by ion-exchange chromatography yielded an active protein fraction, F5, which significantly reduced tumour cell viability *in vitro* and, strikingly, tumour growth *in vivo*. F5 is composed of P1 (peak 1) and P2 subunits interacting in a 1:1 stoichiometric ratio to form a heterotetramer in equilibrium with a hexameric form, which retained biological activity only when assembled. The two peptides share sequence similarity with PIP {PLI-γ [type-γ PLA_2 (phospholipase A_2) inhibitor] from *Python reticulatus*}, existing as a homohexamer. More importantly, although PIP inhibits the hydrolytic activity of PLA_2, the anti-PLA_2 function of F5 is negligible. Using high-resolution MS, we covered 87 and 97 % of the sequences of P1 and P2 respectively. In conclusion, in the present study we have identified and thoroughly characterized a novel protein displaying high sequence similarity to PLI-γ and possessing remarkable cytotoxic and antitumour effects that can be exploited for potential pharmacological applications.

Key words: antitumour activity, apoptosis, *Python sebae*, snake serum, type-γ phospholipase inhibitor (PLIγ).

INTRODUCTION

Little information is available on the identification of antitumour products in snake serum [1]. On the other hand, a variety of factors with cytotoxic activity against murine and human tumour cell lines *in vitro* and antitumour efficacy *in vivo* have been documented in snake venom, and several proteins, including proteases and PLA_2 (phospholipase A_2), have been isolated and characterized [2–7]. To protect themselves from leakage of their own venom PLA_2 proteins into the circulatory system, venomous snakes have PLIs (PLA_2 inhibitors) in their blood, classified into three groups (PLIα, PLIβ and PLIγ) according to their structure and selectivity for specific PLA_2 groups [8,9]. PLIs are acidic oligomeric glycoproteins with N-linked oligosaccharide chains, composed of three to six identical or different non-covalently linked subunits with a molecular mass of 20–30 kDa [10,11]. PLIα is a trimer composed of identical 20 kDa subunits, with a C-type lectin domain, and specifically inhibits group-II acidic PLA_2 proteins. PLIβ selectively inhibits group-II basic PLA_2s and has nine tandem leucine-rich repeats in its sequence. In contrast with PLIα and PLIβ, PLIγ is a rather non-specific inhibitor and its primary structure is characterized by two tandem patterns of cysteine residues, as found in urokinase-type plasminogen activator receptor and in Ly6-related proteins [8,10,12]. All three types of PLIs have been found in the sera of both venomous snakes such as the Viperidae [11] and non-venomous snakes such as *Elaphe quadrivirgata* [13] and *Python reticulatus* [14]. Thus the presence of PLIs in non-venomous snakes suggest that their physiological role might not be restricted to protection against the venom PLA_2s, and that PLIs may exhibit other different, still unknown, functions.

In the present study we have sampled sera from the non-venomous African rock python (*Python sebae*), and tested for cell toxicity and viability, and *in vivo* tumour growth, using several assays. We show that PSS (*P. sebae* serum) produces cytotoxic and antiproliferative effects on tumour cells growing *in vitro* and reduces tumour growth in nude mice transplanted with A431 tumour cells without side effects. To identify the chemical component(s) responsible for its cytotoxic and antitumour activity, PSS was fractionated by ion-exchange chromatography, yielding an active protein fraction (F5). F5 reduced tumour cell viability *in vitro* by inducing apoptosis through a mechanism involving activation of caspase 3, and *in vivo* F5 inhibited A431 xenograft growth in nude mice. Notably, SEC (size-exclusion chromatography) and DLS (dynamic light scattering) measurements revealed that F5 is composed of P1 (peak 1) and P2 subunits interacting in a 1:1 molar ratio to form a tetrameric structure in equilibrium with a hexameric form.

Abbreviations used: a.m.u., atomic mass units; BCA, bicinchoninic acid; CVEC, coronary venular endothelial cell; DLS, dynamic light scattering; DMEM, Dulbecco's modified Eagle's medium; DTT, dithiothreitol; ESI–TOF, electrospray ionization–time-of-flight; FBS, fetal bovine serum; HF, human fibroblast; LAP, leucine aminopeptidase; MALDI–TOF/TOF, matrix-assisted laser-desorption ionization–time-of-flight/time-of-flight; MS/MS, tandem MS; MTT, 3-(4,5-dimethylthiazol-2-yl)-2,5-diphenyl-2*H*-tetrazolium bromide; P, peak; PI, propidium iodide; PLA_2, phospholipase A_2; PLI, PLA_2 inhibitor; PIP, PLIγ from *Python reticulatus*; PRS, *Python regius* serum; PSS, *Python sebae* serum; RP-HPLC, reverse-phase HPLC; S-CM, S-carboxamidomethylated; SEC, size-exclusion chromatography; S-PE, S-pyridylethylated; $sPLA_2$, secretory PLA_2; TB, Trypan Blue; TFA, trifluoroacetic acid; 4VP, 4-vinylpyridine.

[1] To whom correspondence should be addressed (email ziche@unisi.it).

Isolated P1 and P2 lack cytotoxic and antitumour effects. *De novo* sequencing of P1 and P2 reveal that these subunits display high sequence similarity with PIP (PLIγ from *P. reticulatus*) [14]. However, in contrast with PIP, F5 was unable to inhibit PLA_2s.

In conclusion, in the present study we have identified and thoroughly characterized a novel protein displaying high sequence similarity with PLIγ and possessing remarkable cytotoxic and antitumour effects that can be exploited for potential pharmacological applications.

MATERIALS AND METHODS

Python serum sampling

Animal studies were performed in accordance with the European Economic Community guidelines (EEC Law No. 86/609) and the National Ethical Committee. Serum from the subspecies *P. sebae sebae* was sampled from two females aged approximately 3 years. As a control, serum was also sampled from two females of the species *Python regius* aged approximately 3 and 4 years. All donor snakes were born in captivity. Animals were starved for 24 h and sedated by gentle handling for 2 h, then blood samples (average 10 ml) were withdrawn from the cardiac cavity using a 20 cm^3 syringe with a 21-gauge needle. After sedimentation and centrifugation at 1000 ***g*** for 10 min at room temperature (25 °C), the clear supernatant was removed and stored in aliquots at − 20 °C and used in the experiments after appropriate dilution in culture medium or PBS. In the present study, the serum was diluted in culture medium deprived of FBS (fetal bovine serum), and titration was performed by protein content quantified by the Bradford assay. The *P. sebae* serum is identified throughout the paper by the abbreviation PSS, whereas *P. regius* serum is abbreviated as PRS.

Functional assays

Cells and culture conditions

Human squamous epithelial carcinoma (A431), human glioblastoma (U373 MG), human breast cancer (MCF-7) and human fibroblast (HF) cell lines were from the A.T.C.C. The A431 and MCF-7 cell line were cultured in DMEM (Dulbecco's modified Eagle's medium) with 4500 mg/l glucose and 10 % FBS. The HF cell line was cultured in DMEM with 1000 mg/l glucose, 1 % non-essential amino acids, 10 % sodium pyruvate and 10 % FBS. The U373 MG cell line was cultured in MEM (minimal essential medium) with 1 % non-essential amino acids, 10 % sodium pyruvate and 10 % FBS. The mouse lung carcinoma cell line LLC was kindly provided by Dr F. Pica (University of Rome Tor Vergata, Rome, Italy) and was cultured in RPMI 1640 with 10 % FBS. CVECs (coronary venular endothelial cells) were obtained and cultured as described previously [10].

MTT assay

Cell survival was quantified as described previously [15,16] using a Vybrant MTT cell assay kit (Molecular Probes). Briefly, cells (2×10^3 cells/well for CVECs and HF, or 3×10^3/well for A431, MCF-7 and U373MG) were seeded in a 96-well microtitre plate with medium containing 10 % FBS for 5 h, stabilized in 0.1 % FBS for 16 h. Cells were then exposed to different concentrations of PSS for 5 days or to PSS fractions (F1–F6) for 48 h in medium with 1 % FBS. After incubation, cultures were washed with PBS and incubated for 4 h with 1.2 mM MTT [3-(4,5-dimethylthiazol-2-yl)-2,5-diphenyl-2*H*-tetrazolium bromide] in fresh medium. The culture medium was then replaced with an equal volume of DMSO to dissolve formazan crystals. The A_{540} of the formazan was measured using a microplate absorbance reader (Tecan). Cell survival was reported as percentage cell viability = (absorbance of experimental wells × 100)/(absorbance of basal wells).

Apoptosis and necrosis analysis

Bivariant flow cytometry was performed on adherent cells grown in the presence or absence of PSS for 4 h in medium containing 1 % FBS. After incubation, cells were washed in ice-cold PBS and resuspended in 100 μl of binding buffer (Hepes, pH 7, containing 2.5 M $CaCl_2$). Fluorescein-labelled annexin V and PI (propidium iodide) were added to the cell suspension. Annexin V, a member of the calcium- and phospholipid-binding proteins, binds strongly and specifically to phosphatidylserine, which is a marker of cell apoptosis, whereas PI binds to cell DNA, highlighting necrotic cells. Cells were then analysed by flow cytometry (Becton Dickinson) and the results are expressed as the percentage of total cells with positive staining.

In vivo tumour growth

Studies were carried out using 5-week-old female Balb/c nude mice (Harlan Nossan) housed in a barrier care facility and caged in groups of six [17]. Mice were implanted subcutaneously with A431 (1×10^7) cells resuspended in 100 μl of sterile PBS. After 4 days, when the diameter of the tumour mass ranged from 0.5 to 1 mm^3, mice were treated every other day with 100 μl of a solution containing 100 μg of PSS (six mice) or F5 (50 μg/mouse, six mice), injected subcutaneously in proximity to the tumour mass for 12 days. Control mice were treated with PBS (six mice) or with F3 (50 μg/mouse, six mice). Mice were assigned randomly to either group. Tumour dimensions were measured every 2 days with a calliper. Tumour volumes were calculated as width × length × thickness. The survival time of mice was also recorded.

Western blotting

Cells (3×10^5) were seeded in 60 mm-diameter dishes. After adherence, cells were serum-starved (0.1 % serum, 24 h) and then stimulated with F1 or F5 (5 μg/ml) in 1 % FBS. Cells were then lysed and centrifuged at 10000 ***g*** (20 min at 4 °C). A 30 μg portion of proteins were mixed with 4×reducing SDS/PAGE sample buffer and denatured (10 min at 100 °C). Anti-(cleaved caspase 3) antibody was used (1:1000 dilution; Santa Cruz Biotechnology). Results were normalized with actin (1:10000 dilution).

PLA_2 activity assay

The $sPLA_2$ (secretory PLA_2) activity was measured by using an $sPLA_2$ assay kit (Cayman Chemical). Briefly, 1×10^6 A431 cells/100 mm-diameter dish were plated in 10 % FBS for 24 h, and then the conditioned medium was collected, concentrated using Amicon concentrator columns (3 kDa cut-off) and tested for $sPLA_2$ activity in the presence or absence of F5 or F1 following the manufacturer's instructions.

The inhibitory activity of PSS or its fractions was assayed by the $sPLA_2$ (type V) Inhibitor Screening Assay Kit (Cayman Chemical). Briefly, different concentrations of PSS or its cytotoxic fractions were added to the plate containing the $sPLA_2$ and the inhibitory activity was evaluated as A_{405} after 1 min using a plate reader. Data are reported as percentage inhibition for each sample against $sPLA_2$ activity.

Statistics

Results are expressed as means ± S.D. Statistical analysis was performed using Student's *t* test. Differences between groups were considered statistically significant at $P < 0.05$.

Fractionation of PSS

Anion-exchange chromatography

PSS (100 μl), diluted 1:5 in 20 mM Tris/HCl, pH 7.5, and 0.15 M NaCl, was fractionated by ion-exchange chromatography on an FPLC system using a 6 × 60 mm MonoQ anion-exchange column (GE Healthcare) as follows. The serum diluted in Tris/HCl buffer was centrifuged for 2 min at 1000 ***g***, filtered at 0.45 μm on a miniclarifying filter (Millipore) and then applied to the column. The column was equilibrated in 20 mM Tris/HCl, pH 7.5, and 0.15 M NaCl at a flow rate of 0.5 ml/min and eluted with a linear gradient of NaCl from 0.15 to 1.0 M. The A_{280} of the effluent was monitored.

Determination of total protein concentration

The eluted protein material corresponding to the chromatographic peaks was collected, and the protein content was estimated by the Bradford and BCA (bicinchoninic acid) methods. Aliquots of these fractions were tested for cytotoxic and antitumour activities as described above.

RP-HPLC (reverse-phase HPLC)

The fractions eluted at 0.4 M NaCl concentration, denoted as F5 and deriving from several different chromatographic runs, were pooled and freeze-dried. An aliquot (~50 μg) of these fractions was successively solubilized in 0.5 ml of aq. 0.1 % TFA (trifluoroacetic acid) and purified by RP-HPLC on a Vydac C_4 analytical column (The Separation Group) (4.6 × 150 mm, 5 μm particle size). The column was equilibrated with aq. 0.1 % TFA and eluted with a linear acetonitrile/0.1 % TFA gradient from 30 to 60 % in 35 min at a flow rate of 0.8 ml/min. The A_{226} of the effluent was recorded. The presence of two peaks was observed, eluted at approximately 19 and 25 min, which were denoted P1 and P2. These fractions were freeze-dried and subjected to subsequent analyses.

Chemical characterization

Analytical SEC of F5

The apparent molecular mass of fraction F5, eluting at 0.4 M NaCl from the ion-exchange column, was determined by analytical gel-filtration chromatography. Samples were loaded on to a Superose-12 column (1 × 30 cm, GE Healthcare), and eluted with 20 mM Tris/HCl buffer, pH 7.5, at a flow rate of 0.3 ml/min. The column was calibrated using a protein mixture of known molecular mass, in the range 6.5–135 kDa: BSA (67 kDa), ovalbumin (43 kDa), carbonic anydrase (29 kDa), ribonuclease A (13.7 kDa) and aprotinin (6.5 kDa). The interstitial volume (V_i) and the void volume (V_0) were determined by loading the Gly-Tyr-Gly tripeptide and Dextran Blue (2000 kDa) respectively. The distribution constant (K_D) was calculated by the equation $K_D = (V_e - V_0)/(V_i - V_e)$, where V_e is the elution volume of the proteins loaded on to the column.

DLS of F5

DLS measurements on F5 samples (0.7 mg/ml solution filtered at a 0.22 μm cut-off) were carried out at 25 ± 0.1 °C with a Zetasizer Nano S system (Malvern Instruments) at a fixed angle (i.e. 173 °) from the incident light (i.e. a He–Ne 4 mW laser source at 633 nm). ZEN-0117 1 cm pathlength polystyrene cuvettes (100 μl) (Hellma Italia) were used for all measurements. Each measurement consisted of a subset of runs determined automatically, each being averaged for 10 s. Scattering data were analysed with the multimodal algorithm, as implemented in the Nano v. 6.20 software, and presented as the percentage volume size distribution. The refractive index (n) and viscosity (η) of the protein solutions were taken as 1.330 and 0.887 cP.

Electrophoresis

Protein fractions were analysed by gradient gel electrophoresis (SDS/PAGE) using 4–12 % polyacrylamide precast gels. Freeze-dried fractions from anion-exchange chromatography were diluted in 20 μl of gel loading buffer. Samples were then loaded on to the gel, which was run in Tris/glycine buffer, pH 8.3, with 0.1 % SDS. After SDS/PAGE, protein bands were stained by immersing the gel in 0.1 % Coomassie Blue solution in water/methanol/acetic acid (5:4:1) for 30 min and destained by several rinses in 40 % methanol and 10 % acetic acid until a clear background was obtained. To possibly identify carbohydrate chains, protein bands were stained with the GelCode Glycoprotein Staining Kit (Pierce) according to the manufacturer's procedures.

MS and data analysis

For MALDI–TOF/TOF (matrix-assisted laser-desorption ionization–time-of-flight/time-of-flight) analyses, 1 μl of proteolytic digest was deposited on an AnchorChip™ target plate (Bruker Daltonics) and allowed to dry; 0.35 μl of matrix (α-cyano-4-hydroxycinnamic acid; 5 g/l in 1:1 acetonitrile/0.1 % TFA) were then added and, again, allowed to dry. MS analysis was performed on an Ultraflex III MALDI–TOF/TOF instrument (Bruker Daltonics) by using the Flex Control™ 3.0 data acquisition software. Mass spectra were acquired in reflectron mode over the *m*/*z* range 800–5000. The instrumental parameters were chosen by setting the ion source at 25 kV, the reflector at 26.30 kV and the delay time at 20 ns. The instrument was externally calibrated prior to analysis using the Bruker peptide calibrant kit (1046–3147 Da) and the sample spectra were internally recalibrated with trypsin autolysis signals. For MS data acquisition, a total of 400 shots were collected. The peptide masses present in each mass spectrum, through the integrated software Biotools™ 3.0, were used to search the NCBInr databank. Fragmentation of tryptic peptides was obtained using the LIFT™ technology (Bruker Daltonics).

For LC–MS analyses, a Mariner ESI–TOF (electrospray ionization–time-of-flight) instrument (PerSeptive Biosystems) was used. The spray tip potential was set at 3.0 kV, and the nozzle potential and temperature were set at 200 V and 140 °C respectively. Alternatively, MS/MS (tandem MS) analyses were carried out using an Ultimate 3000 instrument (LC Packings Dionex) coupled with an LTQ Orbitrap mass spectrometer (Thermo Fisher Scientific). Peptides were first concentrated on a PepMap100 C_{18} precolumn cartridge [300 μm × 5 mm, 5 μm granulometry, 100 Å porosity (1 Å = 0.1 nm)] from LC Packings Dionex and then eluted on a PepMap100 C_{18} column (75 μm × 15 cm, 5 μm granulometry, 100 Å porosity; LC

Packings Dionex) at a flow rate of 300 nl/min. The mobile phase composition was: 97:3 0.1 % formic acid in H_2O/acetonitrile (phase A), and 97:3 acetonitrile/0.1 % formic acid in H_2O (phase B). The gradient program was: 0 min, 4 % B; 10 min, 40 % B; 30 min, 65 % B; 35 min, 65 % B; 36 min, 90 % B; 40 min, 90 % B; 41 min, 4 % B; 60 min, 4 % B. Mass spectra were acquired in the positive-ion mode, setting the spray voltage at 1.9 kV, the capillary voltage and temperature at 40 V and 200 °C respectively, and the tube lens voltage at 130 V. Data were acquired in the data-dependent mode with dynamic exclusion enabled (repeat count 2); survey MS scans were recorded in the Orbitrap analyser in the mass/charge range 300–2000 *m/z* at a nominal resolution of 15.000, then up to three of the most intense ions in each full MS scan were fragmented and analysed in the Orbitrap analyser at a nominal resolution of 7.500. Singly charged ions did not trigger MS/MS experiments. The acquired data were searched using Bioworks 3.2 (Thermo Fisher Scientific) using Sequest as the search algorithm against all the sequences reported in UniProt for the taxon Python and adding new sequences containing the modifications identified during LIFT experiments. S-carbamidomethylation or S-pyridylethylation was selected as complete modification; two missed cleavages were allowed for trypsin, chosen as the cleaving agent. Searches were performed with a tolerance of 10 p.p.m.

N-terminal sequence analysis

The first 12 amino acids of the purified fractions (P1 and P2) were determined by Edman degradation, carried out by PRIMM, using an automatic protein sequencer (model 477-A, Applied Biosystems).

Determination of cysteine content

Aliquots (100 μg) of RP-HPLC-purified P1 and P2 fractions were subjected to reduction of disulfide bonds and carboxamidomethylation reaction of the cysteine residues, eventually present along the amino acid sequence, to yield the corresponding S-CM (S-carboxamidomethylated) derivatives. The reduction reaction was conducted at 37 °C in 0.1 M Tris/HCl buffer, pH 7.8, 1 mM EDTA and 0.125 M DTT (dithiothreitol). After a 2 h reaction, iodoacetamide was added to a final concentration of 0.25 M and the reaction was allowed to proceed for 90 min at 37 °C. The reaction mixture was then fractionated by RP-HPLC on a C_4 analytical column (4.6 × 150 mm, 5 μm particle size), equilibrated with aq. 0.1 % TFA and eluted with a linear acetonitrile/0.1 % TFA gradient from 30 to 60 % in 35 min, at a flow rate of 0.8 ml/min. Alternatively, P1 and P2 (100 μg each), with cysteine residues in the reduced state, were treated for 90 min at 37 °C with 0.25 M 4VP (4-vinylpyridine) to yield the corresponding S-PE (S-pyridylethylated) derivatives. The reaction was fractionated by RP-HPLC on a C_3 (4.6 × 150 mm, 5 μm particle size) analytical column (Agilent Technologies), eluted with a linear acetonitrile/0.1 % TFA gradient from 10 to 30 % in 5 min and from 30 to 60 % in 40 minutes, at a flow rate of 0.8 ml/min. The A_{226} of the effluent was recorded.

Deglycosylation reaction

Purified P1 or P2 (20 μg) were dissolved in 200 μl of 20 mM sodium phosphate buffer, pH 7.2, containing 100 mM EDTA and 1 % (v/v) 2-mercaptothanol. This solution was treated for 24 h at 37 °C with N-glycosidase F (Roche) (0.2 units of enzyme/mg of protein). The reaction mixture was fractionated by RP-HPLC and analysed by SDS/PAGE. The polyacrylamide gel was stained either with Coomassie Blue or with the GelCode Glycoprotein Staining Kit.

Disulfide reduction and cysteine derivatization of P1 and P2

Reduction of protein (10 μg) disulfide bonds was carried out under denaturing conditions in 0.125 M Tris/HCl buffer, pH 8.3, containing 1 mM EDTA and 6 M GdnHCl (guanidinium chloride) in the presence of a 50-fold molar excess of DTT over the total cysteine content, and incubation was conducted at 56 °C for 90 min. Iodoacetamide was then added at a 10-fold molar excess over the total cysteine content, and the mixture was incubated further in the dark for 60 min at 37 °C. Desalting was carried out on a PD-10 column (GE Healthcare), with elution in 40 mM ammonium bicarbonate buffer. Four 0.5 ml fractions were collected, freeze-dried in a SpeedVac (Thermo Fisher Scientific) concentrator and finally dissolved in 40 μl of 50 mM ammonium hydrogen bicarbonate, pH 7.0. Alternatively, P1 and P2 (100 μg of each), with cysteine residues in the reduced state, were treated for 90 min at 37 °C with 4VP (0.25 M) to yield the corresponding S-PE derivatives. The reaction was stopped by addition of 1 M citric acid solution down to pH 4, and fractionated by RP-HPLC on a C_3 (4.6 × 150 mm, 5 μm particle size) analytical column from Agilent Technologies. The column was eluted with a linear acetonitrile/0.1 % TFA gradient from 10 to 30 % in 5 min and from 30 to 60 % in 40 min, at a flow rate of 0.8 ml/min. The A_{226} of the effluent was recorded.

Tryptic digestion of S-carboxamidomethylated (S-CM-P1 and S-CM-P2) or S-pyridylethylated (S-PE-P1 and S-PE-P2) P1 and P2 subunits

Derivatized proteins (100 μg) were dissolved in 50 mM Tris/HCl, pH 8.0, and 1 mM $CaCl_2$ (200 μl). To this solution, sequencing-grade trypsin (Promega) was added to a final enzyme:protein ratio of 1:20 (w/w). The reaction mixture was incubated at 37 °C overnight, stopped by adding 50 μl of aq. 20 % formic acid, and fractionated by RP-HPLC on a C_{18} analytical column (Agilent Technologies) eluted at a flow rate of 0.8 ml/min with a linear acetonitrile/0.1 % TFA gradient from 5 to 50 % in 40 min. The A_{226} of the effluent was recorded. Eluted peptide material corresponding to the chromatographic peaks was collected, freeze-dried and dissolved in aq. 1 % formic acid for subsequent MS analysis. Cysteine-containing fragments were identified by spectrophotometric analysis of S-PE cysteine in the near-UV region (350–240 nm), using a model Lambda 2 PerkinElmer UV-Vis spectrophotometer.

Subdigestion of tryptic fragments with LAP (leucine aminopeptidase)

P2 tryptic digest was dried in a SpeedVac concentrator and then dissolved in 12 μl of 20 mM Tris/HCl buffer, pH 7.5, containing 1 mM $MgCl_2$. A 5 μl portion of this solution was added to 1 μl of LAP (30 units/μl; Sigma–Aldrich) at room temperature. Aliquots (1 μl) were withdrawn after 1, 2 and 5 min and analysed by MALDI–TOF/TOF or ESI–TOF.

Subdigestion of tryptic fragments with Glu-C endoproteinase

Tryptic fragments that remained unidentified by LC-MS analysis were freeze-dried, dissolved in 100 μl of sodium phosphate buffer, pH 7.8, and treated at 37 °C for 2 h with Glu-C endoproteinase V8 from *Staphylococcus aureus*, using a peptide/protease ratio

of 1:50 (w/w). The reaction was stopped by acid addition and analysed by RP-HPLC on a C_{18} (4.6 × 150 mm) column eluted with a linear acetonitrile/0.1 % TFA gradient from 2 to 60 % in 10 min.

Digestion of S-PE-P1 and S-PE-P2 with Glu-C endoproteinase

Aliquots (100 μg) of derivatized P1 or P2 were dissolved in sodium phosphate buffer, pH 7.8 (200 μl). To this solution, Glu-C endoproteinase V8 (Boehringer) was added to a final enzyme:protein ratio of 1:20 (w/w). The reaction mixture was incubated at 37 °C overnight, stopped by adding 50 μl of aq. 20 % formic acid and fractionated by RP-HPLC. The chromatographic peaks were freeze-dried, dissolved in aq. 1 % formic acid and analysed by ESI–TOF-MS. Prior to mass analysis, all chromatographic fractions were scanned by UV-Vis absorption spectroscopy for identifying S-PE cysteine residues.

Spectroscopic measurements

Protein concentration was determined by the BCA method for both P1 and P2, recording the A_{562} of the solution using a double-beam Lambda-2 spectrophotometer (PerkinElmer). CD spectra were recorded on a Jasco J-810 spectropolarimeter equipped with a thermostatted cell-holder connected to a NesLab RTE-111 water-circulating bath. Far-UV CD spectra were recorded at 20 ± 0.5 °C in 10 mM sodium phosphate, pH 7.0, using a 1 mm-pathlength quartz cell.

RESULTS

PSS induces cytotoxicity in tumour and non tumour cell lines

Cytotoxicity was evaluated in cell suspension as well as on adherent cells. Exposure to PSS in the 50–2000 μg/ml range induced concentration-dependent cytotoxicity in human tumour cell lines (A431 and U373MG, $ED_{50} = 125$ μg/ml; MCF-7, $ED_{50} = 200$ μg/ml), in the mouse tumour cell line LLC ($ED_{50} = 150$ μg/ml) and in the non-tumour cell lines bovine endothelial cells (CVEC; $ED_{50} = 230$ μg/ml) and human skin fibroblasts (HF; $ED_{50} = 250$ μg/ml). (see Supplementary Table S1 at http://www.BiochemJ.org/bj/440/bj4400251add.htm). To investigate the species specificity of PSS activity, we assessed the effect of the serum obtained from two specimens of *P. regius*, PRS1 and PRS2, and from another specimen of *P. sebae*, PSS2. Similar results were obtained with PSS2, whereas PRS1 and PRS2 failed to induce cytotoxic effects (see Supplementary Table S2 at http://www.BiochemJ.org/bj/440/bj4400251add.htm).

PSS reduces cell viability

Microscope observation of cells stained with Diff-Quik after 1 h of exposure to PSS (200 μg/ml) showed that the cytotoxicity was mainly characterized by retraction of cytoplasmic expansion, leading to round-shaped cells and lysis of cell bodies when compared with the basal condition (1 % FBS without PSS) (see Supplementary Figure S1 at http://www.BiochemJ.org/bj/440/bj4400251add.htm). Then, the effects of PSS on cell viability were investigated using the MTT assay. Cells were exposed to PSS for 5 days at concentrations selected as the least toxic, on the basis of previous results in the present study (Table 1). Exposure to repeated PSS treatment (every 2 days for 5 days) in the low-concentration range (20–100 μg/ml), showed that PSS at 20 μg/ml had no relevant effect on cell viability for any cell line. However, at higher concentrations, PSS significantly and concentration-dependently reduced cell viability (Figure 1).

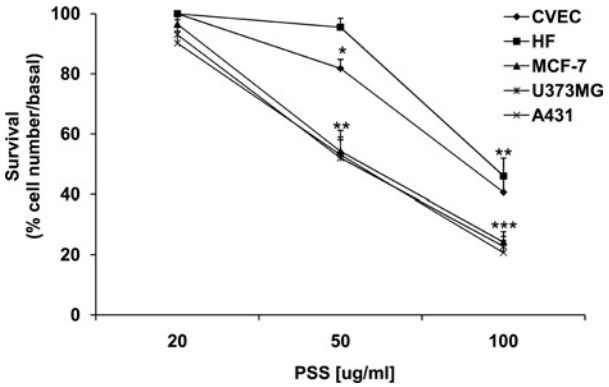

Figure 1 Effect of PSS on cell viability

A panel of tumour and non-tumour cells was used: CVECs, HFs, human breast carcinoma cells (MCF-7), human glioblastoma cells (U373MG) and human squamous cell carcinoma (A431). Cell viability was quantified by an MTT assay after 5 days of exposure to 20, 50 and 100 μg/ml PSS. Results are expressed as percentage cell viability and are the means ± S.D. of three experiments run in triplicate. Basal level = 1 % FBS. $^*P < 0.05$, $^{**}P < 0.01$ and $^{***}P < 0.001$, compared with the basal level.

PSS induces cell apoptosis and necrosis

As shown in Supplementary Figure S1, microscope observations of cells stained with Diff-Quik following PSS treatment documented that the changes were compatible with the occurrence of cell apoptosis and necrosis (retraction of cytoplasmic expansion, rounding of cell shape and lysis of cell bodies). To further investigate the PSS toxicity mechanism and to corroborate the hypothesis that cytotoxicity was mainly associated with cell apoptosis and necrosis, we performed apoptosis/necrosis studies by bivariant flow cytometry analysis using fluorescein-labelled annexin V- and PI-stained cells. The flow-cytometry results of the tumour cell lines A431 and U373MG exposed to different PSS concentrations for 4 h are shown in Table 1. At the maximal PSS concentration tested (200 μg/ml), approximately 50 % of the cells were positive for PI and 30 % were positive for annexin V.

PSS reduces *in vivo* tumour growth

We investigated the effect of PSS treatment on solid tumour growth and overall survival in nude mice. The short supply of the test compound limited the number of animals entering the study. The A431 cell line was selected for *in vivo* experiments. Once A431 cells had produced palpable tumours (4 days after subcutaneous transplant of cells), with the tumour mass ranging between 0.5 and 1 mm^3, treatment with subcutaneous PSS in proximity of the tumour mass was started with a dosing schedule of 100 μg every other day for 12 days. A total of seven treatments was performed. Six control mice, bearing similar tumour masses, were treated only with sterile PBS. PSS treatment was well tolerated, producing neither a local nor a systemic effect. An additional group of mice that received PSS by intraperitoneal injection survived the treatment with no apparent toxic effect (results not shown). PSS treatment reduced A431 tumour growth and, after 6/8 days, the tumour volume was 20 % lower than the control (days 11 and 12 of Figure 2; $P < 0.05$). PSS treatment also affected survival, as four out of six mice survived at day 21, whereas none of the controls survived. However, given the

Table 1 Effect of PSS on cell death

Apoptosis (annexin V-positive cells) and necrosis (PI-positive cells) were measured by FACS analysis after 4 h of exposure of A431 and U373MG cell lines to different concentration of PSS. Results are means ± S.D. for three experiments run in triplicate. $^{**}P < 0.01$ compared with the basal level (0 μg/ml PSS).

PSS (μg/ml)	A431 apoptosis (% annexin V-positive cells)	A431 necrosis (% PI-positive cells)	U373MG apoptosis (% annexin V-positive cells)	U373MG necrosis (% PI-positive cells)
0	9 ± 3	10 ± 4	7 ± 2	8 ± 2
25	8 ± 1	8 ± 2	7 ± 3	27 ± 3**
50	8 ± 3	15 ± 4	7 ± 5	44 ± 11**
100	23 ± 6**	45 ± 5**	24 ± 7**	48 ± 9 **

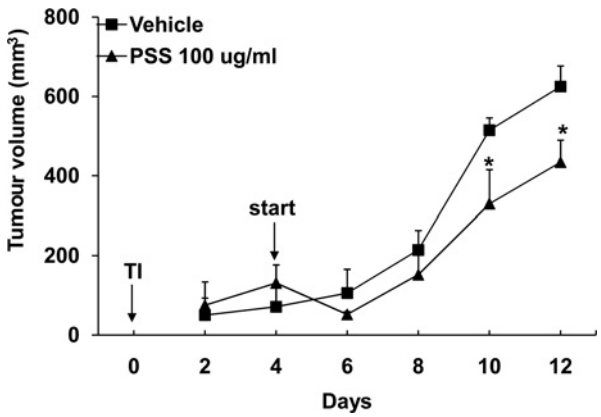

Figure 2 Effect of PSS on A431 tumour cells growing subcutaneously

A431 cells (1×10^6/mouse) were injected subcutaneously in Balb/c nude mice (day 0). PSS (100 μg/100 μl) or vehicle (PBS, 100 μl) was injected every other day subcutaneously close to the tumour mass. Tumour volumes are reported as means ± S.D., $n = 6$. $^{*}P < 0.05$ compared with vehicle. TI, tumour injection.

small number of animals, this difference did not reach significance (results not shown).

Fractionation of PSS and functional characterization of the active component in F5

To purify and further characterize the active component(s) triggering cell death, PSS was fractionated by anion-exchange chromatography (Figure 3A) on a MonoQ column. Aliquots of the protein fractions were analysed by reducing SDS/PAGE (Figure 3A, inset). Fraction F2 contains a minor component at 75 kDa, whereas F3 contains the major component, migrating to 67 kDa, probably corresponding to the snake albumin. Fraction F4 is contaminated by F3 and contains two additional bands at 48 and 35 kDa. Of note, fraction F5 eluting at 0.43 M NaCl contains a highly homogeneous component at ~23 kDa. The concentration of eluted fractions was determined by the BCA assay (see the Materials and methods section) and the effect of each fraction (50 μg/ml final assay concentration) on cell viability was evaluated using the A431, MCF-7 and U373MG tumour cell lines.

As deduced from TB (Trypan Blue) and MTT proliferation assays (Figure 3B), only F5 retained the cytotoxic and anti-proliferative effect of PSS. We then assessed the effect of F5 on the A431 xenograft in nude mice. We compared the antitumour efficacy exerted by F5 (50 μg/100 μl per mouse) with that obtained by administration of F3 or with PBS (100 μl/mouse, control). Tumour growth in the control or F3-treated group proceeded steadily from day 5 increasing up to day 12. Conversely, in animals receiving F5, tumour mass was reduced by approximately 60 % (Figure 3C; $P < 0.05$). In the experimental time frame adopted, neither mortality nor weight loss were observed in any groups.

Furthermore, we investigated the ability of F5 to affect caspase 3 activation, phosphatidylserine expression and tubulin assembly. As shown in Figure 4 and Supplementary Figure S2 at http://www.BiochemJ.org/bj/440/bj4400251add.htm, the cellular effects of F5 appeared to be linked to induction of cell apoptosis, as indicated by caspase 3 activation and phosphatidylserine expression in A431 (Figures 4A and 4B). Conversely, no effect was detected on tubulin assembly, as assessed by immunofluorescence in CVEC, A431 and U373MG cells exposed for 24 h to F5 (50 μg/ml) or, as a positive control, to colchicine (25 μg/ml) (Supplementary Figure S2).

Chemical characterization of the active component F5

Further fractionation of F5 by RP-HPLC (Figure 5A) on a C_4 analytical column yielded two chromatographic peaks of comparable intensity, denoted as P1 and P2, and having molecular mass values of 23135 ± 2 a.m.u. (atomic mass units) and 23152 ± 2 a.m.u. respectively. This small mass difference is consistent with the fact that P1 and P2 of F5 migrated as a single band in SDS/PAGE (see Figure 3A, inset). Notably, when tested for biological activity, both P1 and P2 revealed complete loss of cytotoxic activity (results not shown).

Deglycosylation of disulfide-reduced P2 with N-glycosidase F, which hydrolyses N-linked glycosylation sites at asparagine residues, resulted in a species at 20290.06 ± 5 a.m.u., indicating that the mass contribution of the carbohydrate chain(s) is 2862 a.m.u. In the case of P1, treatment with N-glycosidase F resulted in the precipitation and loss of the protein sample.

The glycoprotein nature of P1 and P2 was confirmed by staining the electrophoretic gel with Coomassie Blue R-250 and with the glycoprotein-specific GelCode staining kit before and after treatment with N-glycosidase F. As expected, the P1 and P2 bands normally stained blue with Coomassie, regardless of glycosidase treatment. Notably, only untreated P1 and P2 stained pink with GelCode. In agreement with the MS data, deglycosylated P1 and P2 bands migrated in SDS/PAGE with a molecular mass 2–3 kDa lower than that of intact proteins (results not shown).

Determination of the cysteine content of the P2 fraction was carried out by a reduction/carboxamidomethylation reaction with DTT/iodoacetamide. The cysteine-reduced and carboxamidomethylated P2 (S-CM-P2) eluted as a single peak in RP-HPLC on a C_4 analytical column (results not shown), with an increase in the mass value of 928.9 ± 0.4 a.m.u. Considering that carboxamidomethylation of half-cystine adds 58.03 a.m.u, we conclude that P2 contains 16 cysteine residues (16×58.03 a.m.u. = 928.48 a.m.u.). Of note, neither P1 nor P2 reacts with

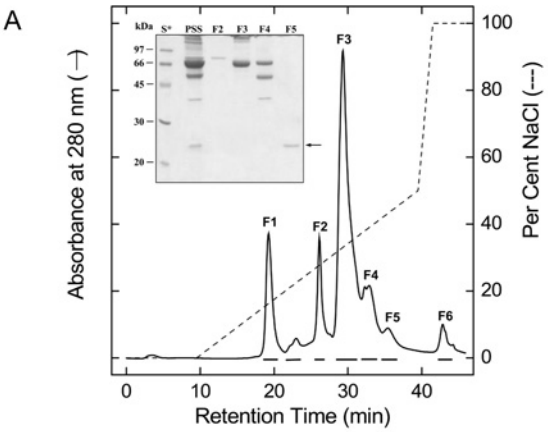

B

	Survival (% Cell Viability)			% Dead cells/Total cells counted		
	A431	MCF-7	U373MG	A431	MCF-7	U373MG
Control	100	100	100	1.4 ± 1.6	2.4 ± 2	3.2 ± 3
F1	119 ± 9			2.2 ± 1.9		
F2	97 ± 20			4 ± 2.7		
F3	90 ± 10	87 ± 15	94 ± 12	3 ± 2.7	2.9 ± 1.7	4.7 ± 4
F4	84 ± 6 *			8 ± 1.7 *		
F5	63 ± 4 **	53± 3 **	58 ± 5 **	14 ± 4 *	21 ± 3.4 *	18 ± 5 *
F6	100 ± 3			2.3 ± 2.9		

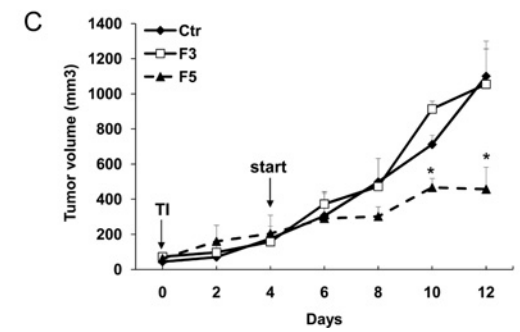

Figure 3 Fractionation of PSS and effect of F1-F6 fractions on *in vitro* tumour cell viability, and *in vivo* tumour growth

(**A**) Fractionation of PSS by anion-exchange chromatography. An aliquot (140 μl) of PSS was loaded on to a MonoQ analytical column, equilibrated in 20 mM Tris/HCl, pH 7.5, containing 0.15 M NaCl at a flow rate of 0.5 ml/min, and eluted with a linear gradient of NaCl from 0.15 to 1.0 M. All fractions were subjected to analysis of total protein content and then tested for cytotoxic antitumoural activity. Inset: SDS/PAGE (12 % gel) of protein fractions eluted from the ion-exchange column. S*, low-molecular-mass protein standard mixture; PSS, crude PSS (0.5 μl); F2–F5, fractions (5 μg/20 μl each). (**B**) Eluted fractions (F1–F6) were tested for their effects on tumour cells. Cell viability was monitored by TB exclusion after 1 h of treatment and by an MTT test after 48 h of treatment. MTT results are expressed as percentage cell viability and are the means ± S.D. of at least two experiments run in triplicate. TB results are expressed as percentage dead cells of total cells counted. Control = 10 % FBS. *$P < 0.05$ compared with control. (**C**) A431 cells (1×10^6/mouse) were injected subcutaneously in Balb/c nude mice. F5 (50 μg/100 μl), F3 (50 μg/100 μl) or vehicle (PBS, 100 μl) was injected every other day subcutaneously close to the tumour mass. Tumour volumes are reported as means ± S.E.M., $n = 6$. *$P < 0.05$ compared with vehicle control (Ctr).

Ellman's reagent [5,5'-dithiobis(2-nitrobenzoic acid)], indicating that no free cysteine residues are present. Similar results were obtained with P1 and P2, after reduction and derivatization with 4VP, a more selective reagent for cysteine residues [18]. In both cases, a mass increment of 1696 ± 0.7 a.m.u. was obtained, thus confirming the presence of 16 cysteine residues in both proteins (106 a.m.u. × 16 = 1696 a.m.u.), arranged to form eight disulfide bonds.

Quaternary structure of the active component F5

As mentioned above, RP-HPLC analysis of F5 shows the presence of two peaks (i.e. P1 and P2) of similar height and area, suggesting that they are represented in F5 in a 1:1 ratio (Figure 5A). However, to discriminate whether P1 and P2 simply co-elute in the F5 fraction during ion-exchange chromatography (Figure 3A) or if they are constitutively associated in F5 to form an oligomeric complex, analytical SEC (Figure 5B) and DLS (Figure 5C) techniques were used. The SEC trace indicate that F5 is conformationally heterogeneous, with a minor species eluting with the void volume, probably corresponding to a high-molecular-mass protein aggregate, and a predominant species eluting with an apparent molecular mass of 87 ± 10 kDa, probably corresponding to a tetramer. A third species elutes as a shoulder with an apparent molecular mass of 123 ± 20 kDa, possibly corresponding to a hexameric form. However, SEC analysis implies dilution of the sample, which can complicate the data interpretation, as concentration-dependent dissociation of the subunits can occur [19].

To overcome this problem, we conducted DLS measurements, where there is no need for sample dilution. In DLS analysis, the time-dependent fluctuations of scattered light from molecules of different size in solution is measured and the rate of these fluctuations is inversely correlated with the molecule size. Generally, an increased hydrodynamic radius (R_H) is obtained for elongated molecules compared with spherical molecules of the same molecular mass. The translational diffusion coefficient (D) was obtained from DLS measurements, whereas R_H was derived from the Stokes–Einstein equation:

$$R_H = \frac{KT}{6\pi\eta D}$$

where K is the Boltzmann constant, T is the absolute temperature and η is the solution viscosity [20]. Thereafter, the molecular mass was estimated using the Protein Utilities tool of the Zetasizer Nano S software. This tool makes use of a calibration curve obtained by plotting the measured R_H value versus the known molecular mass (M_w) of monomeric and oligomeric globular protein standards in the range 17–1120 kDa. The data points in the calibration curve were fitted with the phenomenological equation $R_H = (aM_w)^b$, where a and b are fitting parameters. The size distribution of F5 was first analysed according to the percentage intensity of the scattering molecules, yielding a mean radius (z-average) of 11.02 nm with a quite high PDI (polydispersity index) of 0.40 (results not shown), suggestive of a large conformational heterogeneity of F5 [20]. DLS analysis of F5 is further complicated by the elongated carbohydrate chain(s) accounting for ~14 % of the molecular mass of P1–P2 and protruding outside the protein surface. Considering that at a fixed protein concentration light scattering from large molecules is by far more intense than that from small molecules, the size distribution of F5 was expressed as the percentage volume occupied by the scattering molecules having a certain size. In the latter case, a R_H of 4.91 nm was obtained, with a peak width as large as 2.95 nm (Figure 5C). The R_H value corresponds to an estimated M_w of 139 kDa, fully compatible with the presence of a P1–P2 hexamer. Nevertheless, the value of the peak width limits the possibility to resolve different oligomers having R_H values of the same order of magnitude and is a clear indication of the polydisperse size distribution that can arise from the presence of P1–P2 oligomers existing in equilibrium with each other and from conformational heterogeneity introduced by carbohydrate chains.

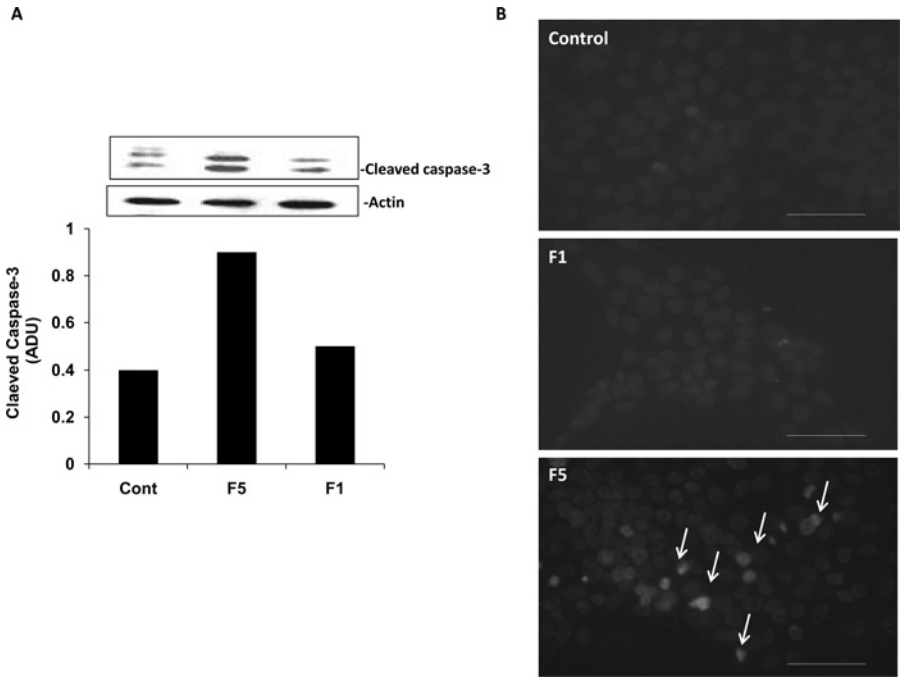

Figure 4 F5 induces cell apoptosis

(**A**) Western blot analysis of cleaved caspase 3 in response to F1 and F5 (50 μg/ml, 24 h). Actin was used for normalization. The histogram represents the quantification of gels. Gels are representative of three experiments with similar results. (**B**) Phosphatidylserine expression on A431 exposed for 24 h to F1 or F5 (50 μg/ml) in 1 % FBS (Control). Scale bar, 50 μm. ADU, arbitrary densitometric analysis units; Cont, control.

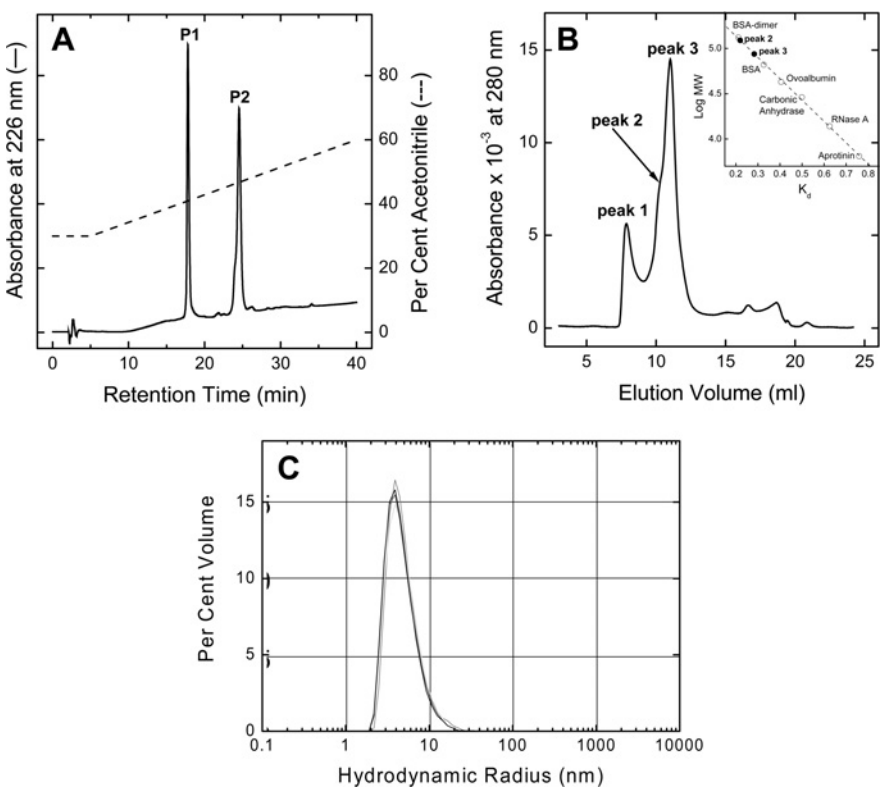

Figure 5 Chemical characterization of F5

(**A**) RP-HPLC analysis of F5. An aliquot (20 μg) of F5 was loaded on to a Vydac (4.6 $\times$ 150 mm) C_4 column eluted with a linear acetonitrile/0.1 % TFA gradient (broken line) at a flow rate of 0.8 ml/min. Two peaks, named P1 and P2, were eluted at 19 and 25 min respectively, and were then collected and subjected to peptide mass fingerprint analysis. (**B**) SEC of F5. F5 aliquots (100 μl) eluted from ion-exchange chromatography (Figure 3A) were loaded on to a Superose-12 column eluted at a flow rate of 0.3 ml/ml and calibrated with suitable protein standards (inset). (**C**) DLS analysis of F5. Measurements were carried out at 25 °C at a protein concentration of 0.7 mg/ml. The size distribution is expressed as the percentage volume occupied by molecules of a certain size.

Altogether, RP-HPLC, SEC and DLS data concurrently suggest that the active fraction F5 is composed of P1 and P2 subunits interacting in a stoichiometric 1:1 ratio to form a tetrameric structure in equilibrium with a hexameric form.

Sequencing P1 and P2 subunits of F5 by peptide mass fingerprint analysis

Although P1 and P2 have very close molecular masses and the same number of cysteine residues, they display very different retention times in RP-HPLC, suggestive of a different amino acid composition or surface charge exposure. This prompted us to undertake the *de novo* sequencing of P1 and P2. HPLC-purified P1 and P2 (see Figure 5A) were subjected to N-terminal sequencing by Edman degradation on a liquid-phase protein sequencer. In both fractions, the sequence HKXEIXHGFGDD was obtained, in which X denotes the absence of a well-defined phenylthiohydantoin amino acid, indicating the presence of a disulfide-bridged cysteine residue in the X position. A BLAST search revealed that the N-terminal sequence HKCEICHGFGDD found in P1 and P2 matched the sequence 1–12, DKCEICHGFGDD, of the $sPLA_2$-inhibitory protein PIP (SwissProt accession number Q9I8P7) [14], except for an amino acid replacement in position 1 (i.e. histidine in *P. sebae* instead of aspartic acid in *P. reticulatus*).

Internal sequence information on P1 and P2 were obtained by peptide mass fingerprinting of reduced and S-alkylated proteins with trypsin and Glu-C endoproteinase after RP-HPLC analysis. Proteolytic peptides eluted at the chromatographic peaks in Supplementary Figure S3 (at http://www.BiochemJ.org/bj/440/bj4400251add.htm) were collected and their accurate mass determined by ESI–TOF or LTQ-Orbitrap MS (Supplementary Tables S3 and S4 at http://www.BiochemJ.org/bj/440/bj4400251add.htm), before and after treatment with N-glycosidase F. Besides accurate MS analysis, cysteine-containing peptides were readily identified by the absorbance spectrum of the S-β-(4-pyridylethyl)-moiety, showing a characteristic shape with a maximum at 254 nm [18], resulting from the appearance of a pyridylethyl fragment ion of 106 a.m.u. in the MS spectrum. In many cases, the chemical identity of proteolytic peptides was also confirmed by MS/MS sequencing in a MALDI–TOF/TOF analysis (see Supplementary Figure S3 and Table S5 at http://www.BiochemJ.org/bj/440/bj4400251add.htm). Notably, some anomalous (e.g. chymotryptic) cleavage was found during proteolysis with trypsin and was confirmed by careful MS/MS analysis.

Glycosylation sites were identified by measuring accurate mass values of the proteolytic peptides shown in Supplementary Figures S3(A) and S3(B) before and after treatment with N-glycosidase F. In the case of P1, the peptide eluting at peak 8 in Figure S3A has a mass of 4391.5 a.m.u. After deglycosylation, the same peptide has a mass of 1528.8 a.m.u, compatible with the P1 fragment 132–144, EENYAG**NIT**YNIK (Supplementary Table S3). Likewise, in the case of P2, the peptide eluting at peak 10 (4419.7 a.m.u.) in Supplementary Figure S3(B) after deglycosylation is converted into a peptide with a mass of 1556.8 a.m.u., corresponding to the P2 fragment 132–144, EENYVG**NIT**YNIK (Supplementary Table S4). In both cases, a mass difference of 2862 ± 0.8 a.m.u. was measured, in excellent agreement with the value measured after deglycosylation of intact P2 (see above). It is noteworthy that, using the NetNGlyc online server (http://www.cbs.dtu.dk/services/NetNGlyc/), Asn^{138} in the NIT sequence (in bold above) of P1 and P2 was identified as a very potent N-glycosylation site. Hence we conclude that P1 and P2 contain a single glycosylation site at Asn^{138}.

From the data reported in the Supplementary Materials and methods section (at http://www.BiochemJ.org/bj/440/bj4400251add.htm) and using the amino acid sequence of PIP from *P. reticulatus* as a template (i.e. 182 amino acids) [14], we identified 159 and 177 amino acids in P1 and P2 respectively, corresponding to a sequence coverage of 87.4 % and 97.2 % (Figure 6). Assignment of the isobaric isoleucine or leucine was on the basis of the template sequence of PIP, which was deduced from the cDNA sequence [14].

Inhibition of PLA_2 activity by F5

Despite the high sequence similarity of P1 and P2 with PIP, F5 exhibited only a modest inhibitory activity on group II $sPLA_2$ from bee venom and on A431-released $sPLA_2$ (Figures 7A and 7B). Furthermore, no effect was observed on group V $sPLA_2$ (Figure 7C).

Conformational characterization

The conformational properties of purified P1 and P2 were investigated by CD in the far-UV region, a spectroscopic technique that provides information on the type of secondary structure content in proteins [21]. The CD spectra of both P1 and P2 (Figure 8) share similar features, with a minimum centred at 212–215 nm, typical of proteins containing a predominantly β-sheet secondary structure [21].

DISCUSSION

In the present study, for the first time, we purified from the serum of the non-venomous snake *P. sebae*, termed PSS, a protein having a selective antitumour activity. PSS cytotoxicity was evaluated in cell suspension and in cell adhesion experiments using both tumour and non-tumour cell lines. In both experimental conditions and for all of the cell lines, PSS exhibited a remarkable and dose-dependent cytotoxic effect. Exposure to a low concentration of PSS for a prolonged time also affected cell viability as measured by the MTT assay. After exposure to PSS at concentrations ranging from 400 to 2000 μg/ml, changes of morphology and cell lysis occurred within minutes. Microscope observation of cells exposed for several hours to PSS evidenced that a consistent proportion of the cell monolayer became detached. The time-dependence of the changes in cell morphology (1 h) is evocative of a rapid treatment-induced gradual loss of cell–matrix adhesion, similar to that documented for other cytotoxic molecules obtained from snakes [22,23]. Consistent with the morphological appearance of cytoplasmic retraction, rounding of cell shape and lysis of cell bodies, PSS effects were mainly associated with cell apoptosis and necrosis. With respect to the decrease in cell viability and the morphological changes observed following exposure to PSS, our results suggest a direct cytotoxic/pro-apoptotic activity of the serum *in vitro*. A key finding of the present study is that the cytotoxic effect appears to be more pronounced in human tumour cells than in non-tumour cells. At a concentration of 50 μg/ml, PSS was devoid of any effect on non-tumour cell lines, while inducing >50 % inhibition of tumour cell growth. These effects were absent at concentrations lower than 50 μg/ml.

In vivo experiments demonstrated that the cytotoxic effect produced *in vitro* on tumour cell lines translated into tumour growth inhibition in nude mice bearing epithelial tumours (A431). PSS peritumoural treatment was well tolerated and reduced tumour growth by 20 %, although this was biased by the limited

```
                    1        10        20        30        40        50        60
P.reticulatus-PIP   DKCEICHGFG DDCDGYQEEC PSPEDRCGKI LIDIALAPVS FRATHKNCFS SSICKLGRVD
P.sebae-P1          HKCEICHGFG DDCDGYEEEC PSPEDKCGKI LIDIALAPVS FRATHKNCFS SSICKLGRVD
P.sebae-P2          HKCEICHGFG DDCDGYQEEC PSPEDKCGKI LIDIALAPVS FRATHKNCFS SSICKLGRVD

                           70        80        90       100       110       120
P.reticulatus-PIP   IHVWDGVYIR GRTNCCDNDQ CEDQPLPGLP LSLQNGLYCP GAFGIFTEDS TEHEVKCRGT
P.sebae-P1          IHVWDGVYMR GRTNCCDNDQ CEDQPLPGLP LSLKNGLYCP GAFGIFTEDS TEHEVKCRGT
P.sebae-P2          IHVWEGVYIR GRTNCCDNDQ CEDQPLPGLP LSLKNGLYCP GAFGIFTEYS TEHEVKCRGT

                          130       140       150       160       170       180
P.reticulatus-PIP   ETMCLDLVGY RQESYAGNIT YNIKGCVSSC PLVTLSERGH EGRKNDLKKV ECREALKPAS SD
P.sebae-P1          ETMCLDLVGY REENYAGNIT YNIKGCVSSC PLLTLSERGH EGRKNDLKKV ECREALKPAS SD
P.sebae-P2          ETMCLDLVGY REENYVGNIT YNIKGCVSSC PLVTLSERGH EGRKNDLKKV ECREALKYES SD
```

Figure 6 Sequence alignment of P1 and P2 from *P. sebae* with PIP from *P. reticulatus*

The amino acids of P1 and P2 that are different in PIP are shaded. The peptide segments of PIP that could not be identified in P1 and P2 are in grey.

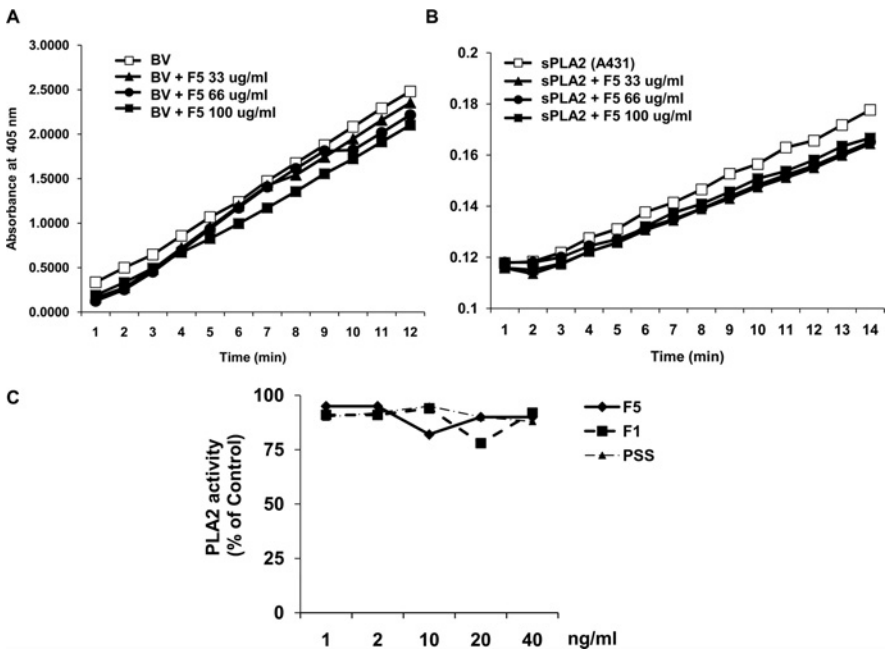

Figure 7 Effect of F5 on PLA_2 activity

(**A**) The effect of F5 was evaluated on group II PLA_2 enzyme activity derived from bee venom (BV) or from PLA_2 enzyme activity released by A431 cultured for 24 h in 10 % FBS. (**B**) The effect of F5 was measured using the $sPLA_2$ assay kit and evaluated by measuring the A_{405}. (**C**) Effect of F1, F5 or PSS on group V $sPLA_2$ enzyme activity. The inhibitory activity of PSS or its fractions was assayed by the $sPLA_2$ (type V) inhibitor screening assay kit and measured as in (**B**). Results are reported as percentage inhibition for each sample compared with sPLA2 activity (reported as 100 %).

number of mice that could be studied given the limited availability of the source. Interestingly, the treatment appeared to increase mouse survival. Given the limited availability of the natural source (i.e. PSS), this finding might be biased by the small number of mice that could be studied. Nevertheless, the effects on tumour growth reduction and increasing mouse survival were significant and appeared worthy of further chemical and functional analysis aimed at isolating the active component responsible for the cytotoxic/antitumour activity of PSS.

The active protein component, F5, was purified from the crude serum by ion-exchange chromatography and its antitumour activity was assessed *in vitro* on several different tumour cell lines and *in vivo* on tumour xenografts. *In vivo*, F5 exhibited potent antitumour effect compared with PSS. Strikingly, after 12 days of treatment, we observed a reduction in tumour size of approximately 60 % in comparison with that measured with buffer alone or with the non-cytotoxic F3 fraction (Figure 3C). Although quite remarkable, the cytotoxicity of F5 (Figure 3B) was not higher than that of the whole python blood serum assayed at the same protein concentration (Figures 1 and 3B). The reduction in the specific activity of bioactive proteins purified from natural sources is not rare. In the present study, this effect could be accounted for by the different physicochemical properties (e.g. pH, ionic strength and viscosity) of the python blood serum compared with those of the purification buffer or the assay medium. These differences or the presence of specific ligands (e.g. lipids) in the serum, which are discarded during purification, might affect the oligomerization state of F5, perhaps promoting the formation of large inactive protein aggregates (see Figure 3A), with a resulting alteration of the biological function.

The results shown in Figure 4 indicate that F5 reduced tumour cell viability and induced apoptosis by activation of the caspase 3 pathway. In an attempt to identify the molecular target of F5, the distribution of β-tubulin was measured in cells treated with the active protein component F5, but no effect was observed on microtubule dynamics. Limitations in the supply of the python blood serum prevented a comprehensive assessment of the putative mechanism for the anti-proliferative activity.

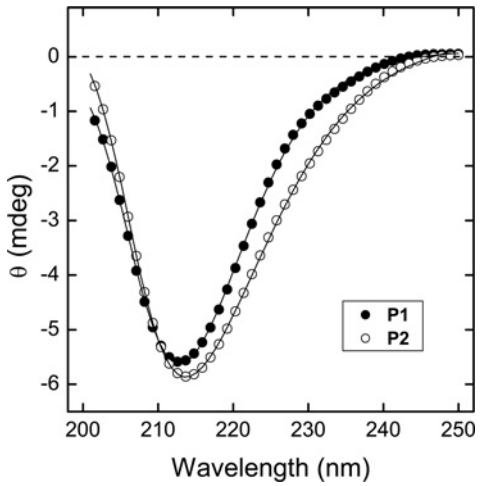

Figure 8 Far-UV CD of P1 and P2

CD spectra were of P1 and P2 were recorded in 10 mM sodium phosphate, pH 7.0, at a protein concentration of 0.17 mg/ml for both proteins. Ellipticity data are expressed as millidegrees without further normalization.

These promising results prompted us to undertake a thorough chemical and conformational characterization of the F5 component. Our results concurrently indicate that F5 is composed of two non-covalently linked protein subunits, P1 and P2, of ~23 kDa each and interacting in a stoichiometric 1:1 ratio to form a predominant heterotetrameric structure existing in equilibrium with a heterohexameric form. Importantly, the PIP inhibitor from *P. reticulatus*, displaying high sequence similarity with P1 and P2, forms a homohexamer [14]. Each subunit in F5 contains a single carbohydrate chain of approximately 3 kDa, N-linked to the conserved Asn^{138}, and 16 cysteine residues arranged to form eight intrasubunit disulfide bridges. The two subunits display high sequence identity and only six mutations could be identified between P1 and P2 (i.e. Glu17Gln, Asp65Glu, Met69Ile, Asp109Tyr, Ala136Val and Leu153Val) (Figure 6). As expected, P1 and P2 also share a similar conformation, characterized by a predominantly β-sheet secondary structure (Figure 8). Interestingly, when purified by RP-HPLC and reconstituted in physiological buffer, the isolated P1 and P2 are still folded but completely lack any biological activity, indicating that the cytotoxic/antitumour function of F5 is inherently associated with the formation of a biologically active F5 oligomer. With respect to this point, the sequence coverage reported in the present study was higher than 87 and 97 % for P1 and P2 respectively. These detailed sequence information will hopefully allow us to isolate, clone and express the gene(s) encoding P1 and P2 in the python genome in order to obtain large protein quantities for further structural and functional analyses.

Another interesting point emerging from the present study is that, despite the absolute conservation of cysteine residues and the high sequence similarity that P1 and P2 display with PIP (Figure 6), F5 has only poor (if any) inhibitory activity toward PLA_2s (Figure 7). This result is even more intriguing if one considers that the peptides that in PIP specify inhibition of PLA_2s (i.e. V^{59}DIHVWDGV^{67} and P^{87}GLPLSLQNG^{96}) [24,25] are also present in P1 and P2 sequences, albeit with a single point mutation in each peptide segment (i.e. Gln94Lys in P1 and P2 and Asp65Glu in P2) (Figure 6). In both cases, however, mutations involve charged amino acids. In addition, comparison of P1 and P2 sequences with that of PIP reveals that, of the eight mutations found in the assigned P1 sequence (i.e. 159 amino acids), four introduce or eliminate an electric charge (i.e. Asp1His, Gln17Glu, Gln94Lys and Gln132Glu). For P2, ten mutations were found out of 177 amino acids assigned. Of these, seven are expected to severely alter the electrostatics or side-chain volume at the mutation site (i.e., Asp1His, Gln94Lys, Asp109Tyr, Gln132Glu, Ala136Val, Pro178Tyr and Ala179Glu). On these grounds, it is not surprising that modification of the surface electrostatic potential of P1 and P2 subunits, caused by mutations, may alter substrate recognition and hinder F5 anti-PLA_2 activity.

In conclusion, in the present study we have shown that PSS contains a previously unknown species-specific and selective cytotoxic protein component endowed with pro-apototic activity and an *in vivo* antitumour effect that could be exploited for the development of novel antitumour strategies.

AUTHOR CONTRIBUTION

Sandra Donnini, Federica Finetti, Simona Francese, Francesca Boscaro, Francesca Dani, Fabio Maset and Roberta Frasson performed experiments, contributed new analytic tools and analysed data. Michele Palmieri, Mario Pazzagli, Vincenzo De Filippis, Enrico Garaci and Marina Ziche designed experiments. Mario Pazzagli, Vincenzo De Filippis, Sandra Donnini and Marina Ziche wrote the paper.

ACKNOWLEDGEMENTS

We thank Francesco Trimigliozzi and Marco Bonazza Foselli for providing python serum samples, and Concetta Montemurno, Mario Granito, Francesco Stannisci, Fiorenzo Refosco and Angela Biscotti for their continuous support during the experimentation. We are indebted to Lucia Morbidelli (Department of Molecular Biology, University of Siena, Siena, Italy) for helping with mouse experiments and cell culture, Gabriella Torcia (Department of Clinical Physiopathology, University of Florence, Florence, Italy) for helping with FACS analysis. This work was inspired by S. Padre Pio da Pietrelcina and is dedicated to him and his teachings.

FUNDING

This work was supported by the Associazione del Bene (Foggia, Italy); and the AIRC (Associazione Italiana per la Ricerca sul Cancro) [grant number IG10731) (to M.Z.).

REFERENCES

1 Thwin, M. M. and Gopalakrishnakone, P. (1998) Snake endovenomation and protective natural endogenous proteins: a mini review of the recent developments (1991–1997). Toxicon **36**, 1471–1482
2 Abu-Sinna, G., Esmat, A. Y., Al-Zahaby, A. A., Soliman, N. A. and Ibrahim, T. M. (2003) Fractionation and characterization of *Cerastes cerastes cerastes* snake venom and the antitumor action of its lethal and non-lethal fractions. Toxicon **42**, 207–215
3 Petretski, J. H., Kanashiro, M. M., Rodrigues, F. R., Alves, E. W., Machado, O. L. and Kipnis, T. L. (2000) Edema induction by the disintegrin-like/cysteine-rich domains from a *Bothrops atrox* hemorrhagin. Biochem. Biophys. Res. Commun. **276**, 29–34
4 Oliveira, J. C., de Oca, H. M., Duarte, M. M., Diniz, C. R. and Fortes-Dias, C. L. (2002) Toxicity of South American snake venoms measured by an *in vitro* cell culture assay. Toxicon **40**, 321–325
5 Schmitmeier, S., Markland, F. S. and Chen, T. C. (2000) Anti-invasive effect of contortrostatin, a snake venom disintegrin, and TNF-α on malignant glioma cells. Anticancer Res. **20**, 4227–423
6 Kini, R. M. (2003) Excitement ahead: structure, function and mechanism of snake venom phospholipase A_2 enzymes. Toxicon **42**, 827–840
7 Koh, D. C. I., Armugam, A. and Jeyaseelan, K. (2006) Snake venom components and their applications in biomedicine. Cell. Mol. Life Sci. **63**, 3030–3304
8 Ohkura, N., Okuhara, H., Inoue, S., Ikeda, K. and Hayashi, K. (1997) Purification and characterization of three distinct types of phospholipase A_2 inhibitors from the blood plasma of the Chinese mamushi, *Agkistrodon blomhoffii siniticus*. Biochem. J. **325**, 527–531
9 Lambeau, G. and Lazdunski, M. (1999) Receptors for a growing family of secreted phospholipases A_2. Trends Pharmacol. Sci. **20**, 162–170

10 Faure, G., Villela, C., Perales, J. and Bon, C. (2000) Interaction of the neurotoxic and nontoxic secretory phospholipases A_2 with the crotoxin inhibitor from *Crotalus* serum. Eur. J. Biochem. **267**, 4799–4808
11 Dunn, R. D. and Broady, K. W. (2001) Snake inhibitors of phospholipase A_2 enzymes. Biochim. Biophys. Acta **1533**, 29–37
12 Ploug, M. and Ellis, V. (1994) Structure–function relationships in the receptor for urokinase-type plasminogen activator. Comparison to other members of the Ly-6 family and snake venom α-neurotoxins. FEBS Lett. **349**, 163–168
13 Okumura, K., Inoue, S., Ikeda, K. and Hayashi, K. (2003) Identification and characterization of a serum protein homologous to α-type phospholipase A_2 inhibitor (PLIα) from a nonvenomous snake, *Elaphe quadrivirgata*. IUBMB Life **55**, 539–545
14 Thwin, M. M., Gopalakrishnakone, P., Kini, R. M., Armugam, A. and Jeyaseelan, K. (2000) Recombinant antitoxic and antiinflammatory factor from the nonvenomous snake *Python reticulatus*: phospholipase A_2 inhibition and venom neutralizing potential. Biochemistry **39**, 9604–9611
15 Donnini, S., Solito, R., Monti, M., Balduini, W., Carloni, S., Cimino, M., Bampton, E. T., Pinon, L. G., Nicotera, P., Thorpe, P. E. and Ziche, M (2009) Prevention of ischemic brain injury by treatment with the membrane penetrating apoptosis inhibitor, TAT-BH4. Cell Cycle **8**, 1271–1278
16 Cantara, S., Thorpe, P. E., Ziche, M. and Donnini, S. (2007) TAT-BH4 counteracts Aβ toxicity on capillary endothelium. FEBS Lett. **581**, 702–706
17 Donnini, S., Finetti, F., Solito, R., Terzuoli, E., Sacchetti, A., Morbidelli, L., Patrignani, P. and Ziche, M. (2007) EP2 prostanoid receptor promotes squamous cell carcinoma growth through epidermal growth factor receptor transactivation and iNOS and ERK1/2 pathways. FASEB J. **21**, 2418–2430
18 Moritz, R. L., Eddes, J. S., Reid, G. E. and Simpson, R. J. (1996) S-pyridylethylation of intact polyacrylamide gels and *in situ* digestion of electrophoretically separated proteins: a rapid mass spectrometric method for identifying cysteine-containing peptides. Electrophoresis **17**, 907–917
19 Corbett, R. J. and Roche, R. S. (1984) Use of high-speed size-exclusion chromatography for the study of protein folding and stability. Biochemistry **23**, 1888–1894
20 Harding, S. E. and Jumel, K. (2001) Light scattering. In Current Protocols in Protein Science (Coligan, J. E., Dunn, B. M., Speicher, D. W. and Wingfield, P. T., eds), Chapter 7, Unit 7.8, John Wiley, New York
21 Brahms, S. and Brahms, J. (1980) Determination of protein secondary structure in solution by vacuum ultraviolet circular dichroism. J. Mol. Biol. **138**, 149–178
22 Baramova, E. N., Shannon, J. D., Bjarnason, J. B. and Fox, J. W. (1989) Degradation of extracellular matrix proteins by hemorrhagic metalloproteinases. Arch. Biochem. Biophys. **275**, 63–71
23 Coelho, A. L., de Freitas, M. S., Oliveira-Carvalho, A. L., Moura-Neto, V., Zingali, R. B. and Barja-Fidalgo, C. (1999) Effects of jarastatin, a novel snake venom disintegrin, on neutrophil migration and actin cytoskeleton dynamics. Exp. Cell. Res. **251**, 379–387
24 Thwin, M. M., Satish, R. L., Chan, S. T. and Gopalakrishnakone, P. (2002) Functional site of endogenous phospholipase A_2 inhibitor from python serum. Eur. J. Biochem. **269**, 719–727
25 Thwin, M. M., Satyanarayanajois, S. D., Nagarajarao, L. M., Sato, K., Arjunan, P., Ramapatna, S. L., Kumar, P. V. and Gopalakrishnakone, P. (2007) Novel peptide inhibitors of human secretory phospholipase A_2 with antiinflammatory activity: solution structure and molecular modeling. J. Med. Chem. **50**, 5938–5950

Received 17 May 2010/5 August 2011; accepted 12 August 2011
Published as BJ Immediate Publication 12 August 2011, doi:10.1042/BJ20100739

Biochem. J. (2011) **440**, 251–262 (Printed in Great Britain) doi:10.1042/BJ20100739

online data

SUPPLEMENTARY ONLINE DATA

A novel protein from the serum of *Python sebae*, structurally homologous to type-γ phospholipase A_2 inhibitor, displays antitumour activity

Sandra DONNINI*, Federica FINETTI*, Simona FRANCESE†, Francesca BOSCARO‡, Francesca R. DANI‡, Fabio MASET§, Roberta FRASSON§, Michele PALMIERI*, Mario PAZZAGLI‖, Vincenzo DE FILIPPIS§, Enrico GARACI¶ and Marina ZICHE*[1]

*Department of Biotechnology and Istituto Toscano Tumori (ITT), University of Siena, Via A. Moro 2, 53100 Siena, Italy, †Biomedical Research Centre, Sheffield Hallam University, Howard Street, Sheffield, S1 1WT, U.K., ‡Mass Spectrometry Center (C.I.S.M.), Viale Pieraccini 6, 50139 Florence, Italy, §Department of Pharmaceutical Sciences, University of Padua, Via F. Marzolo 5, 35130 Padua, Italy, ‖Department of Clinical Physiopathology, University of Florence, Viale Pieraccini 6, 50139 Florence, Italy, and ¶Department of Experimental Medicine and Biochemical Sciences, University of Rome 'Tor Vergata', Viale Regina Elena 299, 00133 Rome, Italy.

SUPPLEMENTARY MATERIALS AND METHODS

Cytotoxicity assay in cell suspension: TB exclusion

Suspensions of the different cell lines (0.5×10^6 cells/ml) were incubated for 1 h in medium with 10 % FBS and various concentrations of PSS. After incubation, the number of dead cells stained by TB was evaluated by optical microscopy. The cytotoxic effects of PSS and PRS were reported as percentage dead cells of total cells counted.

Cytotoxicity assay for cell adhesion: sulforhodamine B assay

Cells (2×10^3 cells/well per 100 μl) were plated in a 96-well microplate containing 10 % FBS for 5 h. After adhesion, the medium was replaced with fresh medium supplemented with 10 % FBS containing different concentrations of PSS and was left on the cells for 1 h. Cells treated with 10 % FBS without PSS represented the basal condition. The supernatant was then discarded and the cells were washed with PBS, fixed for 30 min at 4 °C with 10 % trichloroacetic acid and stained for 30 min with 0.4 % sulforhodamine B in 1 % acetic acid. Unbound dye was removed by four washes with 1 % acetic acid, and protein-bound dye was extracted with 10 mM Tris base for determination of optical density at 564 nm in a computer-interfaced 96-well microtitre plate reader (Tecan). The sulforhodamine B assay results were linear with the number of cells measured by optical microscopy after cell staining with Diff-Quik. Cytotoxicity was reported as percentage dead cells:% dead cells = 100 − (absorbance of experimental wells × 100)/(absorbance of basal wells).

Cell morphology

Cells (3×10^3/well) were plated in a 96-well plate in the presence of 10 % FBS, allowed to adhere for 5 h and then treated with different concentrations of PSS in 10 % FBS for 1 h. Cells (3×10^3/well) were plated in a 96-well plate in the presence of 10 % FBS, allowed to adhere for 5 h, and then treated with different concentrations of PSS in 10 % FBS for 1 h. After supernatant removal, cells were fixed with methanol at 4 °C for 18 h and stained with Diff-Quik. Cell morphology was evaluated by a Nikon Eclipse T400 optical microscope at ×200 magnification and the images were recorded by a Nikon CCD (charge-coupled device) camera. Cell survival was reported as total cell number counted/well.

Immunohistochemical analysis

CVEC, A431 or U373MG cells (2.5×10^4 cells/well on glass coverslips placed into 24-well plates) were incubated in 0.1 % FBS with F5 (50 μg/ml), F1 (50 μg/ml) or colchicine (25 μM). After 24 h, cells were fixed and incubated overnight at 4 °C with monoclonal antibodies against phosphatidylserine (for A431) or α-tubulin (for CVEC, A431 and U373MG) diluted 1:200 in PBS/0.5 % BSA. Samples were then incubated with FITC- or TRITC (tetramethylrhodamine β-isothiocyanate)-conjugated secondary antibodies (Sigma). Markers were assessed by fluorescence microscopy (Eclipse TE300, Nikon) at ×40 magnification and images were captured using a digital camera.

[1] To whom correspondence should be addressed (email ziche@unisi.it).

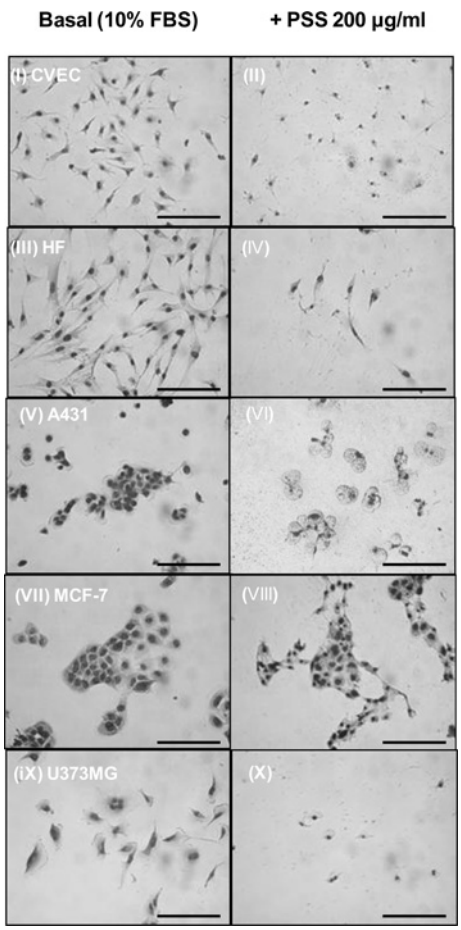

Figure S1 Cytotoxic effect of PSS on tumour and non-tumour cells

Cell morphology of tumour and non-tumour cell lines after a 1 h exposure to PSS was evaluated following staining with Diff-Quik. Cells were treated with 10% FBS or with 10% FBS in the presence of 200 μg/ml PSS for 1 h (CVEC, panels I and II; HF, panels III and IV; A431, panels V and VI; MCF-7, panels VII and VIII; and U373MG, panels IX and X respectively). Cell morphology was evaluated using a Nikon Eclipse T400 optical microscope and the images were recorded using a Nikon CCD camera at the end of the incubation time. Scale bar, 20 μm.

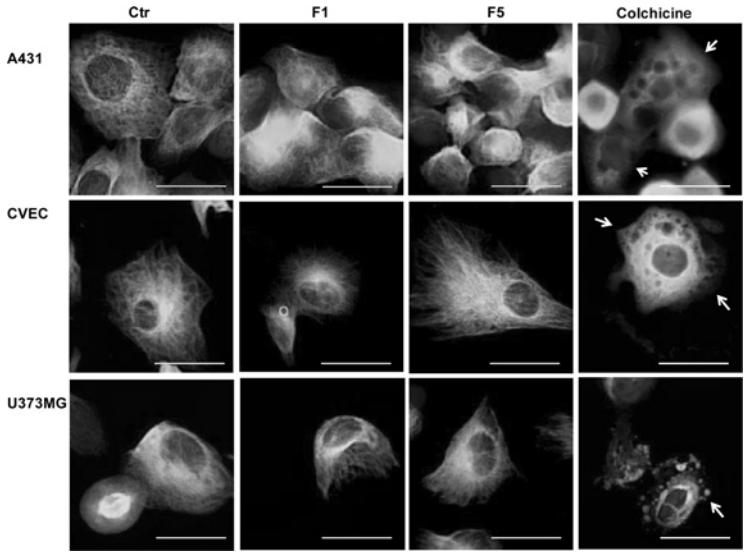

Figure S2 Effect of F5 on α-tubulin assembly

α-Tubulin morphology in CVEC, A431 and U373MG cells exposed for 24 h to F1 or F5 (50 μg/ml) in 1 % FBS (control, Ctr). Colchicine was used as a positive control (25 μM). Arrows show cell bubbles. Scale bar, 50 μm.

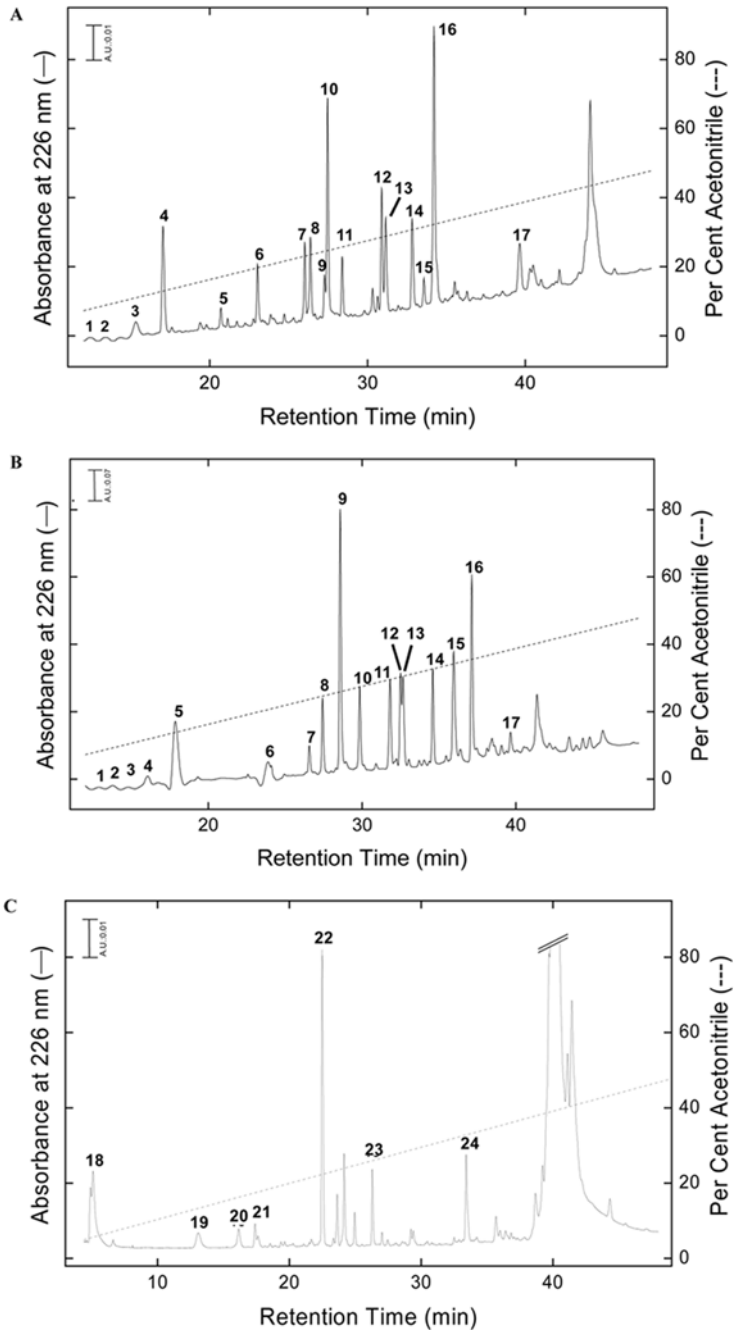

Figure S3 Proteolysis of S-PE derivatives of P1 and P2 with trypsin and Glu-C endoproteinase

RP-HPLC analysis of P1 (**A**) and P2 (**B**) with trypsin. (**C**) RP-HPLC analysis of P2 with Glu-C protease.

Table S1 Cytotoxic effect of PSS

Cytotoxicity was measured by (a) TB exclusion (cells in suspension) and (b) sulforhodamine B assay (adherent cells). Cells were exposed to serial dilutions of PSS for 1 h at 37 °C in medium containing 10 % FBS. Results are expressed as the percentage dead cells of the total number of cells counted and are means ± S.D. of four experiments run in duplicate. $^{*}P < 0.05$, $^{**}P < 0.01$ and $^{***}P < 0.001$ compared with basal.

(a) TB assay (% dead cells of total cells counted)

PSS (μg/ml)	CVEC	HF	A431	U373MG	MCF-7	LLC
0	5 ± 2	3 ± 1	7 ± 2	8 ± 5	6 ± 2.4	6 ± 3
2000	99 ± 5***	96 ± 6***	100 ± 0***	100 ± 0***	95 ± 6***	98 ± 1***
800	96 ± 3***	87 ± 5***	98 ± 1***	100 ± 0***	90 ± 8.3***	98 ± 0***
400	86 ± 7***	70 ± 8***	94 ± 2***	99 ± 1***	91 ± 3***	95 ± 3***
200	21 ± 5**	33 ± 6**	88.6 ± 5***	80 ± 5***	51 ± 8**	77 ± 6***
100	12 ± 9	9 ± 4	45 ± 9*	42 ± 11*	24 ± 3*	28 ± 11*
50	6 ± 4	5 ± 3	20 ± 8*	17 ± 5*	15 ± 0.4*	4.2 ± 3

(b) Sulforhodamine B assay (% dead cells of total cells counted)

PSS (μg/ml)	CVEC	HF	A431	U373MG	MCF-7
0	10 ± 2	13 ± 1	7 ± 2	9 ± 5	10 ± 2.4
2000	55 ± 3**	50 ± 2**	95 ± 5***	79 ± 5***	82 ± 6***
400	35 ± 2*	30 ± 3*	84 ± 7***	67 ± 4***	70 ± 5***
200	16 ± 2	14 ± 6	48 ± 3**	53 ± 5**	50 ± 4**

Table S2 Effect of sera sampled from two *Python* species on cytotoxicity

Cytotoxicity was measured by the TB exclusion assay. Cell suspensions were exposed to sera obtained from two different *P. sebae* (PSS and PSS2) and *P. regius* (PRS1 and PRS2) animals for 1 h at 37 °C in medium containing 10 % FBS. Results are expressed as the percentage dead cells of the total number of cells counted and are means ± S.D. of four experiments run in duplicate. $^{*}P < 0.05$, $^{**}P < 0.01$ and $^{***}P < 0.001$ compared with basal. ND, not done.

Serum concentration (μg/ml)	CVEC	HF	A431	U373MG	MCF-7
PSS					
0	5 ± 2	3 ± 1	7 ± 2	8 ± 5	6 ± 2.4
400	86 ± 7***	70 ± 8***	94 ± 2***	98 ± 1***	90 ± 2***
100	12 ± 9	9 ± 4	45 ± 9*	42 ± 11*	ND
PSS2					
0	6 ± 3	4 ± 3	8 ± 1	6 ± 1	6 ± 2
400	79 ± 7***	78 ± 16***	96 ± 4***	87 ± 3***	91 ± 3***
100	10 ± 5	15 ± 7	37 ± 4*	35 ± 10*	24 ± 3*
PRS1					
0	5 ± 3	4 ± 3	7 ± 5	8 ± 6	5 ± 2
400	2 ± 2	26 ± 11	17 ± 6	17 ± 7	15 ± 5
100	4 ± 4	6 ± 4	5 ± 4	0.5 ± 0.3	5 ± 4
PRS2					
0	4 ± 2	5 ± 2	6 ± 3	3 ± 3	9 ± 1
400	2 ± 2	7 ± 5	14 ± 4	4 ± 2	10 ± 8
100	2 ± 2	3 ± 2	0.8 ± 1.6	2 ± 3	4 ± 0.6

Table S3 Mass data of P1 digest with trypsin

Peak number*	Experimental mass (a.m.u.)†	Theoretical mass (a.m.u.)†	Mass difference (a.m.u.)	Position	Sequence deduced (mutations in bold)	Mutation(s)‡
1	382.50	382.48	+ 0.02	117–118	CR	
2	616.34	616.35	− 0.01	164–168	KNDLK	
3	738.38	738.38	0.00	169–173	KVECR	
4	656.27	656.27	0.00	98–103	YCPGAF	
5	1192.24	1192.32	− 0.08	19–29	ECPSPED**K**CGK	R26K
6	2717.18	2717.23	− 0.05	73–94	TNCCDNDQCED QPLPGLPLSL**K**	Q94K
7	1197.54	1197.53	+ 0.01	47–55	NCFSSSICK	
8	1528.79	1528.70	+ 0.08	132–144	**E**E**N**YAG**D**ITYNIK§	Q132E, S134N, N138D
9	2106.51	2106.55	− 0.04	3–18	CEICHGFGDDCDGY**E**E	Q17E
10	3489.46	3489.35	+ 0.11	3–29	CEICHGFGDDCDGY**E**E ECPSPED**K**CGK	Q17E, R26K
11	1490.61	1490.69	− 0.08	104–116	GIFTEDSTEHEVK	
12	1673.75	1673.83	− 0.08	145–158	GCVSSCPL**L**TLSER	V153L
13	1045.48	1045.47	+ 0.01	95–103	NGLYCPGAF	
14	1561.77	1561.73	+ 0.04	119–131	GTETMCLDLVGYR	
15	1488.76	1488.72	+ 0.04	59–70	VDIHVWDGVY**M**R	I69M
16	1033.57	1033.62	− 0.05	85–94	PLPGLPLSL**K**	Q94K
17	1426.86	1426.85	+ 0.01	30–42	ILIDIALAPVSFR	

*Peak numbers refer to the peaks eluted from the RP-HPLC column in Supplementary Figure S3A.
†Experimental and theoretical mass values refer to the mono-isotopic species.
‡Mutated residues in P1 compared with PIP from *Python reticulatus*.
§The substitution N138D is artefactual and originates from glycosidase-mediated hydrolysis of the amide bond formed by the Asn^{138} side chain and the carbohydrate chain.

Table S4 Mass data of P2 digest with trypsin and GluC

Peak number*	Experimental mass (a.m.u.)†	Theoretical mass (a.m.u.)†	Mass difference (a.m.u.)	Position	Sequence deduced (mutations in bold)	Mutation(s)‡
Trypsin						
1	382.51	382.48	− 0.03	117–118	CR	
2	616.33	616.35	− 0.02	164–168	KNDLK	
3	459.27	459.27	0.00	174–177	EALK	
	610.29	610.29	0.00	170–173	VECR	
4	738.38	738.38	0.00	169–173	KVECR	
5	656.27	656.27	0.00	98–103	YCPGAF	
6	1040.43	1040.47	− 0.04	174–182	EALK**YE**SSD	P178Y, A179E
7	488.23	488.26	− 0.03	165–168	NDLK	
8	1197.53	1197.53	0.00	47–55	NCFSSSICK	
9	3490.98	3490.90	+ 0.08	3–29	CEICHGFGDDCDGYQ EECPSPED**K**CGK	R26K
10	1556.82	1556.74	+ 0.08	132–144	**E**E**N**Y**V**G**D**ITYNIK§	Q132E, S134N A136V, N138D
11	1659.85	1659.81	+ 0.04	145–158	GCVSSCPLVTLSER	
12	1634.81	1634.77	+ 0.04	43–55	ATHKNCFSSSICK	
13	1539.62	1539.66	− 0.04	104–116	GIFTE**Y**STEHEVK	D109Y
14	1561.74	1561.73	+ 0.01	119–131	GTETMCLDLVGYR	
15	2719.15	2719.12	+ 0.03	73–94	TNCCDNDQCEDQPLP GLPLSL**K**	Q94K
16	1484.76	1484.78	− 0.02	59–70	VDIHVW**E**GVYIR	D65E
17	1426.82	1426.85	− 0.03	30–42	ILIDIALAPVSFR	
Glu-C endoprotease						
18	511.23	511.22	+ 0.01	172–174	CRE	
19	620.28	620.27	+ 0.01	1–4	**H**KCE	D1H
20	896.44	896.45	− 0.01	115–121	VKCRGTE	
21	1185.69	1185.68	+ 0.01	162–171	GRKNDLKKVE	
22	622.32	622.33	− 0.01	175–179	ALK**YE**	P178Y, A179E
23	1896.71	1896.70	+ 0.01	5–19	ICHGFGDDCDGYQEE	
24	1532.74	1532.70	+ 0.04	122–133	TMCLDLVGYR**E**E	Q132E

*Peak numbers refer to the peaks eluted from the RP-HPLC column in Supplementary Figure S3(B) (i.e. trypsin cleavage) and Supplementary Figure S3(C) (i.e. cleavage by Glu-C protease).
†Experimental and theoretical mass values refer to the mono-isotopic species.
‡Mutated residues in P2 compared with PIP from *P. reticulatus*.
§The substitution N138D is artefactual and originates from glycosidase-mediated hydrolysis of the amide bond formed by the Asn^{138} side chain and the carbohydrate chain.

Table S5 LTQ-Orbitrap and MALDI–TOF/TOF analysis of the tryptic P2 digest

Experimental mass (a.m.u.)*	Theoretical mass (a.m.u.)*	Mass difference (a.m.u.)	Position	Peptide sequence‡	Mutation(s)†
1426.862	1426.862	0.000	30–42	ILIDIALAPVSFR	
987.423	987.423	0.000	47–55	NCFSSSICK	
1810.991	1810.992	− 0.001	56–70	LGRVDIHVW**E**GVYIR	D65E
1484.784	1484.785	0.001	59–70	VDIHVW**E**GVYIR	D65E
2461.133	2461.133	0.000	95–116	NGLYCPGAFGIFTE**Y**STEHEVK	D109Y
3052.431	3052.423	+ 0.008	119–144	GTETMCLDLVGYR**E**E **N**Y**V**G**D**ITYNIK	Q132E, S134N, A136V, N138D
1556.751	1556.743	+ 0.008	132–144	**EE**N**Y**V**G**D**I**TYNIK	Q132E, S134N A136V, N138D
1563.776	1563.746	+ 0.030	145–158	GCVSSCPLVTLSER	
616.362	616.362	0.000	164–168	KNDLK	
1103.583	1103.583	0.000	164–173	KNDLKKVECR	
1040.473	1040.473	0.000	174–182	EALK**YE**SSD	P178Y, A179E

*Experimental and theoretical mass values refer to the mono-isotopic species.
†Mutated residues in P2 compared with PIP from *P. reticulatus*.
‡Bold residues refer to mutations.

Received 17 May 2010/5 August 2011; accepted 12 August 2011
Published as BJ Immediate Publication 12 August 2011, doi:10.1042/BJ20100739